



## Visualization of nanofibrillar cellulose in biological tissues using a biotinylated carbohydrate binding module of -1,4-Glycanase

Knudsen, Kristina Bram; Kofoed, Christian; Espersen, Roall; Højgaard, Casper; Winther, Jakob R.; Willemoës, Martin; Wedin, Irene; Nuopponen, Markus; Vilske, Sara; Aimonen, Kukka; Weydahl, Ingrid Elise Konow; Alenius, Harri; Norppa, Hannu; Wolff, Henrik; Wallin, Erik Håkan Richard; Vogel, Ulla

*Published in:*

Chemical Research in Toxicology

*DOI:*

[10.1021/acs.chemrestox.5b00271](https://doi.org/10.1021/acs.chemrestox.5b00271)

*Publication date:*

2015

*Document version*

Publisher's PDF, also known as Version of record

*Citation for published version (APA):*

Knudsen, K. B., Kofoed, C., Espersen, R., Højgaard, C., Winther, J. R., Willemoës, M., ... Vogel, U. (2015). Visualization of nanofibrillar cellulose in biological tissues using a biotinylated carbohydrate binding module of -1,4-Glycanase. *Chemical Research in Toxicology*, 28(8), 1627-1635. <https://doi.org/10.1021/acs.chemrestox.5b00271>

## Visualization of Nanofibrillar Cellulose in Biological Tissues Using a Biotinylated Carbohydrate Binding Module of $\beta$ -1,4-Glycanase

Kristina Bram Knudsen,<sup>†</sup> Christian Kofoed,<sup>‡</sup> Roall Espersen,<sup>‡</sup> Casper Højgaard,<sup>‡</sup> Jakob Rahr Winther,<sup>‡</sup> Martin Willemoës,<sup>‡</sup> Irene Wedin,<sup>§</sup> Markus Nuopponen,<sup>||</sup> Sara Vilske,<sup>⊥</sup> Kukka Aimonen,<sup>⊥</sup> Ingrid Elise Konow Weydahl,<sup>†</sup> Harri Alenius,<sup>⊥</sup> Hannu Norppa,<sup>⊥</sup> Henrik Wolff,<sup>⊥</sup> Håkan Wallin,<sup>†,#</sup> and Ulla Vogel<sup>\*,†,○</sup>

<sup>†</sup>National Research Centre for the Working Environment, Lersø Parkallé 105, DK-2100 Copenhagen Ø, Denmark

<sup>‡</sup>Section for Biomolecular Sciences, Department of Biology, University of Copenhagen, Copenhagen, DK-2200 N, Denmark

<sup>§</sup>Stora Enso, FI-00100 Helsinki, Finland

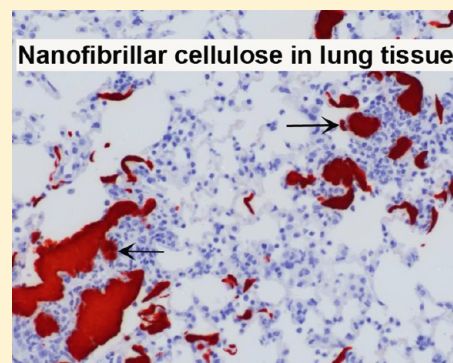
<sup>||</sup>UPM Kymmene Oyj, FI-00100 Helsinki, Finland

<sup>⊥</sup>Nanosafety Research Centre, Finnish Institute of Occupational Health, P.O. Box 40, FI-00250 Helsinki, Finland

<sup>#</sup>Institute of Public Health, Copenhagen University, Øster Farimagsgade 5, Copenhagen K, Denmark

<sup>○</sup>Department of Micro- and Nanotechnology, DTU, Kgs. Lyngby, Denmark

**ABSTRACT:** Nanofibrillar cellulose is a very promising innovation with diverse potential applications including high quality paper, coatings, and drug delivery carriers. The production of nanofibrillar cellulose on an industrial scale may lead to increased exposure to nanofibrillar cellulose both in the working environment and the general environment. Assessment of the potential health effects following exposure to nanofibrillar cellulose is therefore required. However, as nanofibrillar cellulose primarily consists of glucose moieties, detection of nanofibrillar cellulose in biological tissues is difficult. We have developed a simple and robust method for specific and sensitive detection of cellulose fibers, including nanofibrillar cellulose, in biological tissue, using a biotinylated carbohydrate binding module (CBM) of  $\beta$ -1,4-glycanase (EXG:CBM) from the bacterium *Cellulomonas fimi*. EXG:CBM was expressed in *Escherichia coli*, purified, and biotinylated. EXG:CBM was shown to bind quantitatively to five different cellulose fibers including four different nanofibrillar celluloses. Biotinylated EXG:CBM was used to visualize cellulose fibers by either fluorescence- or horse radish peroxidase (HRP)-tagged avidin labeling. The HRP-EXG:CBM complex was used to visualize cellulose fibers in both cryopreserved and paraffin embedded lung tissue from mice dosed by pharyngeal aspiration with 10–200  $\mu$ g/mouse. Detection was shown to be highly specific, and the assay appeared very robust. The present method represents a novel concept for the design of simple, robust, and highly specific detection methods for the detection of nanomaterials, which are otherwise difficult to visualize.



### INTRODUCTION

Nanofibrillar cellulose (also called nanocellulose) is a dense network of highly fibrillated celluloses ranging from 10 to 100 nm in diameter and several micrometers in length.<sup>1,2</sup> Nanofibrillar cellulose constitutes an innovation potential within the forest sector since nanofibrillar cellulose can be used as high strength materials in products such as high quality paper, coatings, cosmetics, vehicles, furniture, food, electronic components, and pharmaceuticals. Recently, the production of nanofibrillar cellulose on an industrial scale has become economically feasible.<sup>1,3,4</sup> Because of their mechanical properties and low production costs, nanofibrillar cellulose constitutes an attractive alternative to other nanofibers, e.g., carbon nanotubes.<sup>4,5</sup> Nanofibrillar cellulose is produced by the mechanical refining of wood or natural fiber pulp, followed by either grinding or homogenization.<sup>2</sup>

Workers exposed to cotton dust, which principally consists of cellulose, have been reported to develop chest tightness, hyperresponsiveness, and chronic bronchitis.<sup>6</sup> Exposure to wood dust (where cellulose is the major constituent) causes cancer of the nose and the paranasal sinuses,<sup>7</sup> and exposure to textile fibers in weavers has also been considered possibly carcinogenic.<sup>8,9</sup> Cellulose fibers have been shown to persist in the lungs of rats with a half-life in the range of 1000 days after intratracheal deposition.<sup>9</sup> Workers may be exposed to airborne nanofibrillar cellulose particles from grinding or spray drying during production.<sup>1</sup> However, data on health effects in workers exposed to nanofibrillar cellulose are at present largely unavailable.<sup>1</sup> There are reasons for health concern related to

Received: May 12, 2015

Published: July 24, 2015

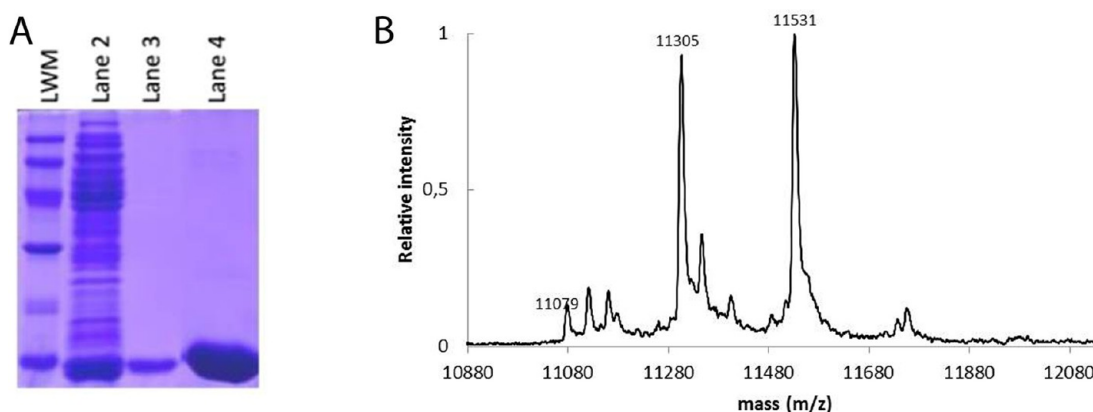


**Figure 1.** Production and purification of EXG:CBM (A) and MALDI-TOF evaluation of the biotinylation of EXG:CBM (B). (A) SDS-PAGE gel of crude *E. coli* extract from cells producing EXG:CBM and subsequent purification with Avicel. Lane 1: molecular weight marker (phosphorylase b (97 kDa), albumin (66 kDa), ovalbumin (45 kDa), carbonic anhydrase (30 kDa), trypsin inhibitor (20.1 kDa), and  $\alpha$ -lactalbumin (14.4 kDa)). Lane 2: cell lysate loaded equivalent to 200  $\mu$ L of induced culture. Lane 3: cell lysate equivalent to 2 mL of induced culture incubated with 3 mg of Avicel and washed. Lane 4:  $\sim$ 50  $\mu$ g of EXG:CBM after the last purification step. (B) Biotinylation of EXG:CBM. Labeling of EXG:CBM ( $M_w = 11079$  Da) using the biotinylation reagent biotin-NHS in 12-fold molar excess at pH 7.0 resulted in a modification of the protein's two available amino groups. Masses correspond to modification of either the N-terminus or the side chain of Lys28 ( $M_w = 11305$  Da) or both ( $M_w = 11531$  Da). Nearby peaks stem from adduct ions.

**Table 1. Characteristics of the Five Different Cellulose Fibers (CF) Used in the Study**

material	concentration (%)	fiber length (nm)	fiber width (nm)	aspect ratio	zeta potential (mV)	remarks
CF1	2.40	2000–20 000	2–15	100–1000	–15	enzymatic pretreatment
CF2	1.60	2000–50 000	3–10	100–5000	–32	carboxy-methylated
CF3	0.79	500–10 000	4–10	100–1000	–25	biocide 12,5 ppm (BIM MC 4901), carboxylated
CF4	1.47	2000–20 000	7–20	100–2000	–2	
CF5	4.30					bulk-sized

nanofibrillar cellulose since they, like asbestos and carbon nanotubes, are high aspect ratio materials, and exposure could cause physiological responses (e.g., inflammation) in the respiratory tract. Studies of nanomaterial toxicity are often hampered by difficulties in detecting and quantifying the nanomaterial in biological tissues. This is especially true for carbon-based nanomaterials and biological nanomaterials like nanofibrillar cellulose, which mainly consists of glucose moieties.

Exoglucanases (EXG) bind cellulose with very high specificity and affinity via the cellulose binding domain EXG:CBM.<sup>10</sup> We have utilized the specific binding properties of EXG:CBM to develop a new detection method for the visualization of cellulose fibers. Here, we show that biotinylated EXG:CBM can be used to visualize pulp cellulose as well as four different types of nanofibrillar cellulose fibers in biological tissue, that biotinylated EXG:CBM can be used on both cryopreserved and paraffin embedded lung tissues, and that specific staining can be obtained using both fluorescence- and horse radish peroxidase (HRP)-tagged avidin labeling.

## METHODS

**Production and Purification of EXG.** The plasmid pJexpress401:22788 carries the coding sequence corresponding to the 110 amino acid long EXG:CBM [PDB: 1EXG] from the gene *Cex* ( $\beta$ -1,4-glycanase from the bacterium *Cellulomonas fimi*). The structure of the EXG:CBM protein has been solved by NMR.<sup>11</sup> EXG:CBM contains a disulfide bond, and to ensure correct disulfide bond formation, the PelB signal peptide sequence from *Pectobacterium carotovorum* was fused to the reading frame encoding EXG:CBM in order to target EXG:CBM to the periplasm. The reading frame, including the signal peptide, was custom synthesized by DNA2.0 (Menlo Park, CA, USA) in a vector, pJexpress401 (DNA2.0), under control of the T5 promoter and with

kanamycin resistance as the selection marker. The codon bias of the EXG:CBM reading frame was optimized for expression in *Escherichia coli* according to the algorithms of DNA2.0. EXG:CBM was produced from the plasmid pJexpress401:22788 in *E. coli* strain MAS72 (*rec*<sup>+</sup> derivative of MAS90).<sup>12</sup> MAS72 was grown at 37 °C in buffered rich medium supplemented with salts<sup>13</sup> and 30  $\mu$ g/mL kanamycin. EXG:CBM synthesis was induced by the addition of isopropyl  $\beta$ -D-1-thiogalactopyranoside (IPTG) to the growth media to a final concentration of 0.1 mM at a cell culture density of OD<sub>600</sub> = 1, and the cultures were left to grow for 20 h at 37 °C. Cells were harvested, washed, and resuspended in 50 mM Tris-HCl and 1 mM EDTA at pH 7.0. A sequence of 20 s sonication at 40% maximum energy (an amplitude of 8  $\mu$ m) on a Soniprep 150 (Sanyo) sonicator, followed by a 60 s pause while kept on ice released the protein from the periplasm into the supernatant. Cell debris was removed by centrifugation at 20,000g for 20 min at 4 °C. Protein yields of EXG:CBM from 1 L culture, grown as above, were typically 15–20 mg.

EXG:CBM was purified taking advantage of the affinity of the protein for cellulose<sup>10</sup> by incubating the cell lysate with 1 g (dry weight) of Avicel (Sigma-Aldrich) per liter original culture with agitation for 1 h at 25 °C. The Avicel with bound EXG:CBM was pelleted by centrifugation at 5,000g for 20 min at room temperature, and the supernatant was discarded.

The Avicel pellet was packed in a Pharmacia XK 16 column with a thermostatic jacket and washed with three column volumes of 1 M NaCl followed by the same amount of water. To elute the protein, the temperature of the column was ramped up from 70 to 82 °C during 20 min, while continuously running water over the column (2 mL/min). EXG:CBM was eluted, and fractions containing protein (as determined by absorbance at 280 nm) were collected and lyophilized. After dissolving in water, insoluble material was pelleted by centrifugation as described above. The yield of EXG:CBM at this point was typically 80–90%, and the protein was more than 95% pure as judged by SDS-PAGE (Figure 1A, lane 3). However, when performing assays

Table 2. Binding Data for EXG to the Different Types of Cellulose

	$K_{D1}$ ( $\mu\text{M}$ )	$B_{max1}$	$K_{D2}$	$B_{max2}$
CF2	$0.0063 \pm 0.0023$	$1.46 \pm 0.17$	$0.65 \pm 0.28$	$2.47 \pm 0.28$
CF1	$0.010 \pm 0.0055$	$1.33 \pm 0.22$	$0.72 \pm 0.31$	$2.03 \pm 0.19$
CF3	$0.022 \pm 0.0062$	$2.28 \pm 0.35$	$0.76 \pm 0.56$	$2.36 \pm 0.37$
CF4	$0.055 \pm 0.0083$	$2.69 \pm 0.09$	-	-
CF5	$0.084 \pm 0.017$	$3.24 \pm 0.17$	-	-
nylon filter	$0.35 \pm 0.054$	$1.07 \pm 0.038$	-	-

Binding constants ( $K_D$ ) and maximum binding ( $B_{max}$ ) and (-) indicate that only a one-site binding model was used for fitting. Data were fitted to a two-site binding model, when this was appropriate.

for carbohydrate content using the phenol-sulfuric acid method,<sup>14</sup> the EXG:CBM preparation at this stage consistently revealed a slight carbohydrate (cellulose) contamination (equivalent to about 1 mole glucose monomer per mole EXG:CBM).

To remove trace elements of cellulose and reagents from the labeling reaction, fractions were applied to a Pharmacia Superdex 75 size-exclusion column using 100 mM ammonium hydroxide (pH 8.5) as mobile phase, and the protein fractions were pooled and lyophilized. The yield of EXG:CBM was 70–75% at this final stage.

The purity of EXG:CBM in the different steps of the purification procedure is shown in Figure 1A. It should be noted that EXG:CBM is retained on Superdex 75 most likely due to a slight affinity for the column material and elutes after the column volume. No carbohydrate was detected in EXG:CBM samples from this step. After an additional lyophilization, the protein was stored as powder and dissolved in water or a proper buffer just before use and centrifuged as above to pellet any insoluble material.

**EXG:CBM Biotinylation.** To biotinylate EXG:CBM, a 30 mM stock solution of NHS-biotin (Thermo Scientific) was made freshly in DMSO and was added in 12-fold molar excess to 1 mg/mL EXG:CBM in 20 mM sodium phosphate (pH 7.0). The reaction was incubated for 5 h at 25 °C with stirring after which the reaction was quenched by the addition of 1 M Tris-HCl to a final concentration of 10 mM. The biotinylated EXG:CBM was separated from the reaction mixture by Superdex 75 gel-filtration as described above.

**MALDI-TOF MS.** EXG:CBM samples were prepared by dilution in 0.1% trifluoroacetic acid (TFA) to a concentration of 1  $\mu\text{M}$ . Fresh matrix was prepared by thoroughly mixing sinapinic acid with a 1:1 (v/v) solution of 0.1% TFA and acetonitrile. Any undissolved sinapinic acid was pelleted by centrifugation for 15 min at 15,000g. Equal volumes of the resulting supernatant and the diluted EXG:CBM samples were mixed and spotted on the steel target. Crystallized spots were analyzed in a Bruker Autoflex MALDI-TOF mass spectrometer, using a laser power intensity of 64.75  $\mu\text{J}$ . The spectra obtained were normalized to the highest intensity recorded.

**Measurement of Cellulose Binding by EXG:CBM.** The method was based on a depletion assay for EXG:CBM.<sup>15</sup> Two-hundred and fifty  $\mu\text{L}$  binding reactions were made by mixing 200  $\mu\text{L}$  of the prepared stock of cellulose fiber (250  $\mu\text{g}/200 \mu\text{L}$ ) and 50  $\mu\text{L}$  of varying concentrations of EXG:CBM in binding buffer (50 mM sodium phosphate, pH 6.5) and incubated for 1 h while shaking. Samples from the incubations were then transferred to 0.2  $\mu\text{m}$  spin-filters (modified nylon VWR Centrifugal Filter, art. no. 516-0234) and centrifuged at 10,000g for 2 min. The filtrate was collected, and 450  $\mu\text{L}$  of binding buffer was added. Binding of EXG:CBM to the nylon membrane of the spin-filters was determined in a binding experiment performed as described above with the omission of cellulose fibers in the incubation. The EXG:CBM concentration remaining in the filtrate was determined on a PerkinElmer LS 55 luminescence spectrometer based on two standard curves: one determined for 0.0075–0.1  $\mu\text{M}$  EXG:CBM at a slit width of 2.5 nm for excitation and 10 nm for emission and one determined for 0.1–2.5  $\mu\text{M}$  EXG:CBM at a slit width of 2.5 nm for excitation and 2.6 nm for emission. The latter standard curve was verified by absorbance measurements at 280 nm. Both standard curves showed that the intensity was linearly dependent on protein concentration with  $R^2 > 0.99$  for both lines.

**Analysis of Binding Data.** Results from binding experiments were analyzed using the OriginLab 9.1 software by fitting the built in equations for one-site binding or two-site binding isotherms to the data:

$$\text{one-site binding: } [bound] = \frac{B_{max}[L]}{K_D + [L]}$$

$$\text{two-site binding: } [bound] = \frac{B_{max1}[L]}{K_{D1} + [L]} + \frac{B_{max2}[L]}{K_{D2} + [L]}$$

where  $[bound]$  is the concentration of EXG:CBM bound to the cellulose and removed from the sample during centrifugation.  $B_{max}$  is the calculated concentration of binding sites in the sample.  $[L]$  designates the free EXG:CBM concentration obtained in the sample that passed through the spin filter (see above procedure). The data analysis was performed after subtracting the binding of EXG:CBM binding to the nylon membrane of the spin-filters.

**Celluloses.** Four nanofibrillar cellulose materials (denoted CF1–CF4) and one bulk-sized cellulose fiber (denoted CF5) were used in the study. All cellulose samples were derived from natural wood-based pulp, and they consisted of glucose, xylose, and mannose. Material characteristics are presented in Table 1. The materials were produced and provided by Stora Enso Oyj and UPM Kymmene Oyj. Physicochemical characteristics of the cellulose fibers were provided by the manufacturers. Fiber length was determined by scanning electron microscopy (Zeiss Model EVO MA 10) and laser diffraction (Horiba LA 950). Fiber width was determined by atomic force microscopy (Cypher System, Asylum Research). Zeta potential was determined by dynamic light scattering (Malvern Zetasizer Nano).

**Dispersion of Celluloses.** Cellulose dispersions were prepared in phosphate buffered saline (PBS, Lonza, Basel, Switzerland). The amount of cellulose needed was either measured with a 1 mL syringe (SOFT-JECT Insulin U-100) or weighed due to high viscosity of the material. Cellulose was dispersed in PBS by high speed vortexing for 10 min to yield a 4 mg/mL stock dispersion. Further dilutions were prepared from the stock dispersion by a dilution series, followed by vortexing for 10 min. Immediately before administration, the dispersions were vortexed quickly.

**Animals.** Female C57BL/6 mice were obtained from Scanbur AB (Karlslunde, Denmark) and quarantined for 1 week. The mice were 7–8 weeks old at arrival and were housed in groups of 4 mice per cage in humidity- and temperature-controlled ventilated rooms with a 12 h day/night cycle. Rodent diet (Altromin no. 1314 FORTI, Altromin Spezialfutter GmbH & Co., Germany) and water were provided *ad libitum*. Cage-side clinical observations were conducted on a daily basis during the study.

Mice in groups of 8 were exposed to 10, 40, 80, or 200  $\mu\text{g}$  of each of CF material in a 50  $\mu\text{L}$  volume (corresponding to 0.2, 0.8, 1.6, or 4 mg/mL dispersions) by single pharyngeal aspiration. Since PBS was used as vehicle, mice in the control group were exposed to 50  $\mu\text{L}$  of PBS. The mice were sacrificed by an overdose of isoflurane 24 h after exposure. A slice from the left lung was fixed in formalin, while another slice from the left lung was embedded in O.C.T. compound (optimal cutting temperature) (TissueTek, Sakura, The Netherlands) and snap frozen on dry ice.



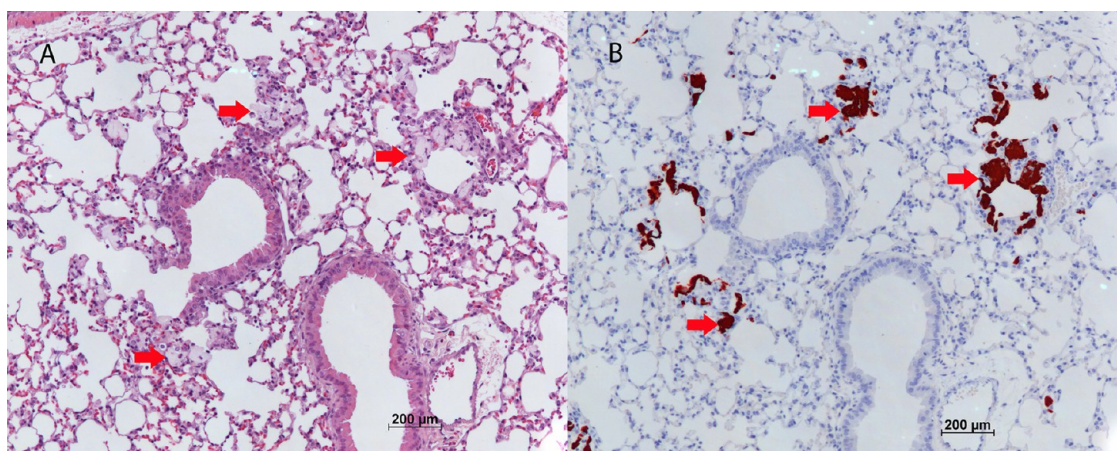


**Figure 2.** Specific staining of CF1 with EXG:CBM in paraffin embedded lung tissue sections from mice exposed to CF1. (A) H&E staining of paraffin embedded lung tissue from mice exposed to 200  $\mu\text{g}$  of CF1. Microscope objective  $\times 10$ . Arrows locate unstained cellulose fibers. (B) Serial section of the same tissue as in panel A stained with biotinylated EXG:CBM conjugated to HRP, counterstained with Mayer's hematoxylin. Arrows locate cellulose fibers identified by the EXG:CBM staining.

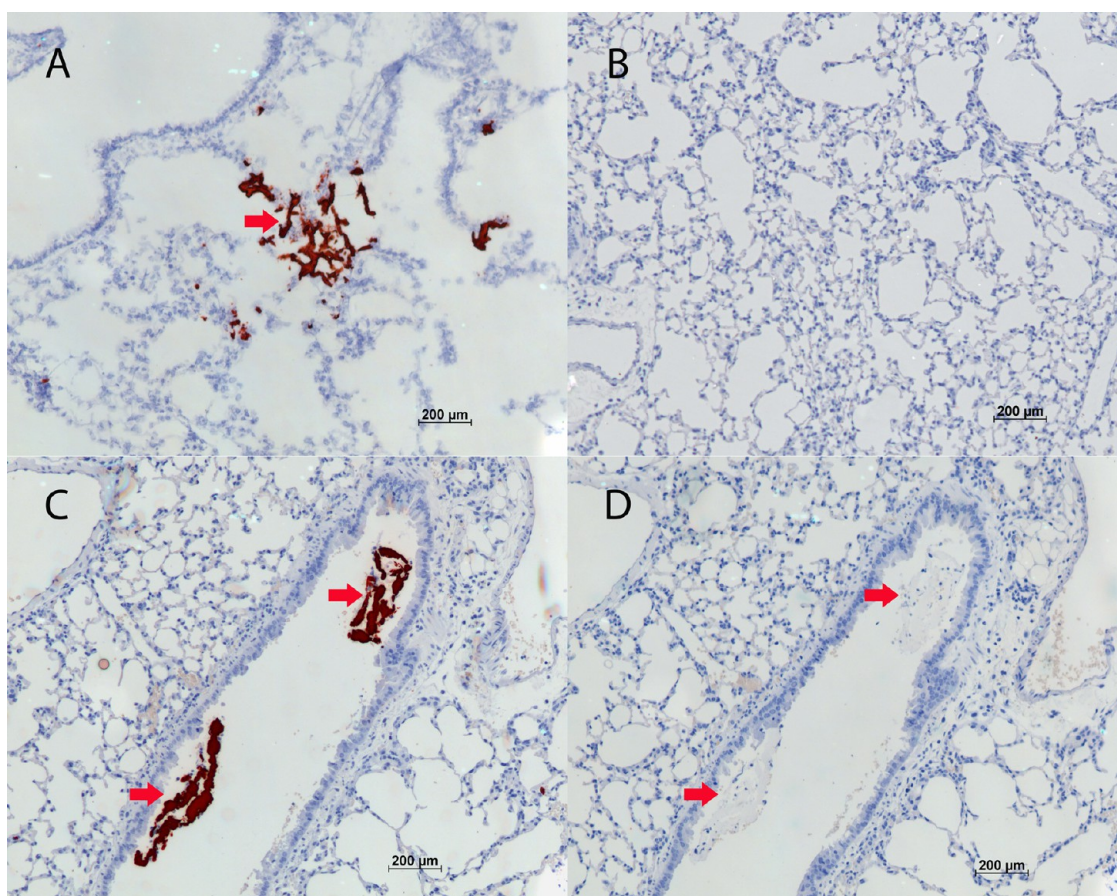


**Figure 3.** Specific staining of CF1 with biotinylated EXG:CBM in paraffin embedded and cryopreserved lung tissues, counterstained with Mayer's hematoxylin. (A) Cryopreserved lung sections from mice exposed to 200  $\mu\text{g}$  of CF1 stained with biotinylated EXG:CBM. Microscope objective 10 $\times$ . Arrows locate cellulose fibers identified by the EXG:CBM staining. (B) Paraffin embedded tissue from vehicle (PBS) exposed mice stained with biotinylated EXG:CBM. Microscope objective 10 $\times$ . (C) Paraffin embedded lung tissue from mice exposed to 200  $\mu\text{g}$  of CF1. Microscope objective 10 $\times$ . Arrows locate intrabronchially located cellulose fibers identified by the EXG:CBM staining. (D) Control staining of a serial section of the same tissue as that in panel C stained using the immunohistochemistry protocol but excluding biotinylated EXG. Arrows locate unstained cellulose fibers. Microscope objective is 10 $\times$ .

The study was approved by the Animal Experiment Board and the State Provincial Office of Southern Finland.

**Histology and Immunohistochemistry.** The formalin fixed samples were trimmed, dehydrated, and embedded in paraffin. Sections

from both formalin fixed and frozen tissues were cut at 3  $\mu\text{m}$  on a Microtome (Leica Microsystems, Wetzlar, Germany). For general morphology, the sections were stained with hematoxylin and eosin (H&E) stain.



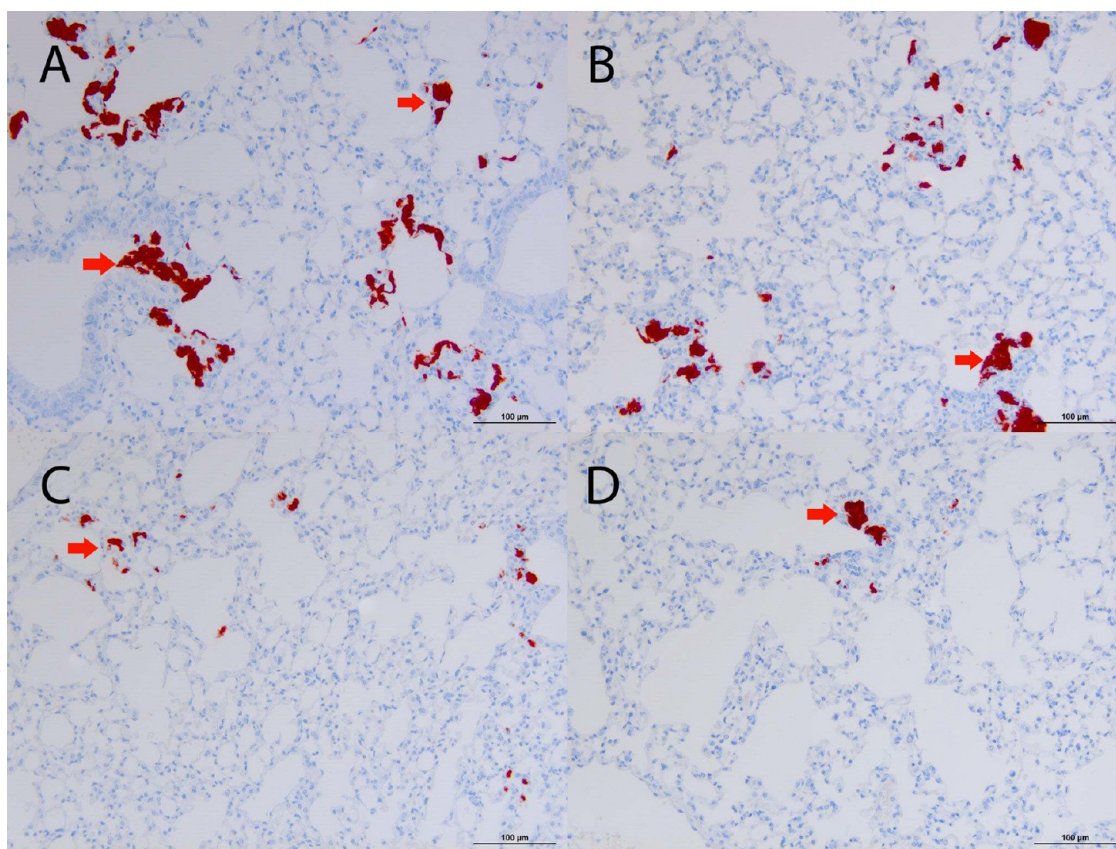


**Figure 4.** HRP-EXG:CBM staining of lung sections from mice dosed with different amounts of CF1. Paraffin embedded lung sections were stained with biotinylated EXG:CBM and counterstained with Mayer's hematoxylin. Microscope objective is 20 $\times$ . A, 200  $\mu$ g of CF1; B, 80  $\mu$ g of CF1; C, 40  $\mu$ g of CF1; and D, 10  $\mu$ g of CF1. Arrows locate cellulose fibers identified by the EXG:CBM staining.

For EXG:CBM staining, frozen sections were fixed in acetone for 5 min, or paraffin was removed from the sections, and the sections were washed with PBS. Endogenous peroxidase was blocked with Ultravision Hydrogen Peroxide Block (Thermo scientific, Fremont CA, USA) for 10 min. After washing with PBS, 30% rabbit normal serum with avidin from Avidin/Biotin Blocking kit, Vector Laboratories (Burlingame, CA, USA) was applied to the sections for 30 min and then removed by gentle suction. Biotinylated EXG (final dilution 1:300 with biotin from Avidin/Biotin Blocking kit) was applied to the sections for 60 min. After washing with PBS, Streptavidin Peroxidase Conjugated (Rockland, Limerick, PA, USA) was applied to the sections for 30 min at a dilution of 1:300. After washing in PBS, peroxidase enzyme activity was visualized by incubation in Large Volume AEC Chromogen Single Solution (Thermo Scientific) for 5 min. The sections were then counterstained with Mayer's hematoxylin, dried and mounted.

**Fluorescence Staining for Cellulose.** For fluorescence staining, tissue sections (from paraffin or OCT) were blocked with avidin from Avidin/Biotin Blocking kit, Vector Laboratories (Burlingame, CA, USA) in 2% rat serum in nanopure water for 10 min. The slides were then blocked with biotin from Avidin/Biotin Blocking kit for 10 min. Then, biotinylated EXG (diluted 1:300 final concentration) was applied to the sections for 60 min. After washing in PBS, avidin FITC conjugate (ImmunoPure Avidin, Fluorescein Conjugated, Thermo Scientific) was added to the slides for 30 min in the dark. After washing, the slides were mounted and analyzed.

## RESULTS

**Protein labeling.** EXG:CBM has two potential biotinylation sites, the *N*-terminus and the  $\epsilon$ -amine of lysine 28. Successful biotin-labeling was indicated by the increased masses of EXG:CBM of 226 or 452 Da, respectively, detected by MALDI-TOF MS,

indicating single and double biotinylation along with a small signal from unlabeled EXG:CBM (Figure 1B).

**Celluloses.** Four nanofibrillar cellulose materials (denoted CF1–CF4) and one bulk-sized cellulose fiber (denoted CF5) were used in the study (Table 1).

**EXG:CBM Binding to Nanofibrillar Cellulose.** Cellulose fibers CF1–CF5 were assayed for EXG:CBM binding capability (Table 2). EXG:CBM showed strong binding to CF2 ( $K_{D1} = 6.3 \pm 2.3$  nM), and the binding was best fitted to a two-site binding model. Both the low  $K_D$  and the two-site binding previously have been observed for EXG:CBM, when binding to crystalline cellulose, like Avicel.<sup>15</sup>

The four other cellulose fibers were tested for their ability to bind EXG. Cellulose fibers CF1 and CF3 showed EXG binding characteristics similar to those of CF2 but with slightly lower affinity for EXG:CBM (Table 2). The two remaining cellulose fibers (CF4 and CF5) could not be fitted to a two-site binding model. The calculated binding affinity was about 10-fold lower for CF4 and CF5 compared to that of the high affinity site on CF2; therefore, we propose that the  $K_D$  for the second binding site was too high to be detected in our binding assay. Biotinylation had no effect on the affinity of EXG:CBM for any of the tested celluloses (results not shown).

**Tissue Staining of Cellulose with EXG:CBM Protein.** Four different types of nanofibrillar cellulose and one bulk cellulose were deposited into the lungs of mice by aspiration, and the mice were sacrificed after 24 h. Biotinylated EXG:CBM bound to avidin-HRP was used to visualize cellulose fibers in lung tissue. CF1 was faintly visualized in lung tissue by H&E



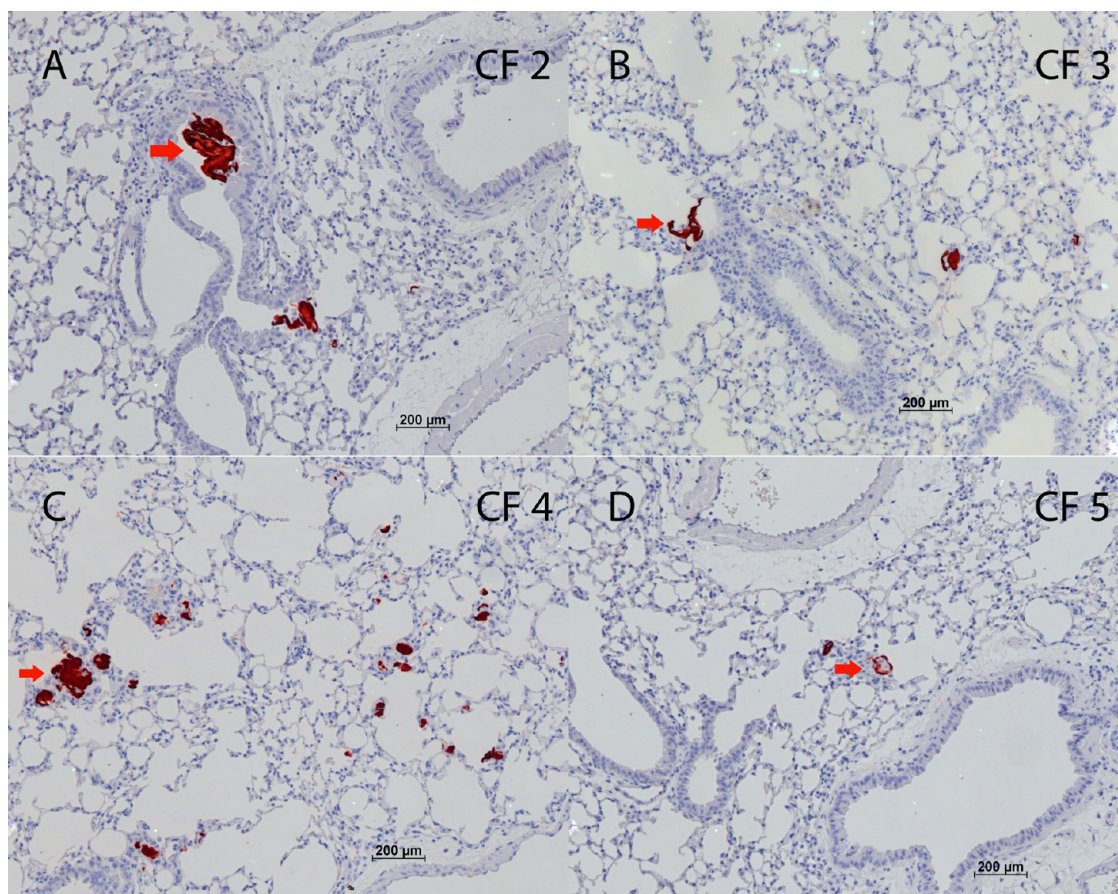


**Figure 5.** HRP-EXG:CBM staining of paraffin embedded lung sections from mice exposed to 40  $\mu\text{g}$  of cellulose fibers and counterstained with Mayer's hematoxylin. Microscope objective is 10 $\times$ . A, CF2; B, CF3; C, CF4; and D, CF5. Arrows locate cellulose fibers identified by the EXG:CBM staining.

staining (Figure 2A) and clearly visualized following incubation with biotinylated EXG:CBM followed by avidin conjugated to HRP (Figure 2B). The HRP staining appeared as dark red spots in the alveolar sacs/ducts. EXG-HRP staining of CF1 was also demonstrated on cryopreserved lung tissue from mice dosed with CF1 by aspiration (Figure 3A). Specificity was demonstrated by the lack of HRP staining in EXG:CBM-stained lung tissue from the vehicle-exposed mice (Figure 3B) and by the lack of HRP staining when CF1-exposed lung tissue was stained with avidin conjugated to HRP in the absence of biotinylated EXG:CBM (Figure 3D), versus staining with the presence of EXG:CBM from the same series of sections (Figure 3C), thus confirming that there was no nonspecific binding of HRP-avidin.

Mice were exposed to 200, 80, 40, and 10  $\mu\text{g}$  of CF1 (Figure 4A–D) to assess the sensitivity of the HRP-EXG:CBM staining visualized in lung sections. The five different CF materials were all visualized in lung tissue by EXG:CBM-HRP staining. Thus, CF2 (Figure 5A), CF3 (Figure 5B), CF4 (Figure 5C), and CF5 (Figure 5D) were readily visualized with HRP-EXG:CBM.

EXG:CBM was also visualized with fluorescence using FITC conjugated to avidin. Again, a highly specific staining was detected in paraffin embedded lung tissue from mice exposed by aspiration to CF1 (Figure 6A). The CF1 in Figure 6A was faintly visible under light microscopy (Figure 6B). No signal was detected in lung sections from vehicle exposed mice (Figure 6C). EXG:CBM was also visualized with fluorescence in cryopreserved tissue slides from mice exposed to CF3 (Figure 7A) and CF1 (Figure 7B).

## DISCUSSION

The understanding of how exposure is related to biodistribution and the internal dose is crucial in the evaluation of adverse effects of hazardous agents. In nanotoxicology, detection of nanomaterials in biological tissues is often hampered either by high background levels (e.g., zinc oxide, iron oxide, and others) or by the lack of sensitive and specific detection methods of the nanomaterials. Nanomaterials may be visualized using electron microscopy provided that they are electron dense<sup>16,17</sup> or may be recognized by their specific structures.<sup>18,19</sup> Other detection methods such as dark field hyperspectral microscopy have been used to visualize nanomaterials.<sup>20–22</sup> We have taken an alternative approach and utilized the specific binding properties of a CBM of a cellulose degrading enzyme to develop highly specific visualization of cellulose fibers.

We demonstrate that the detection method can be used to detect and visualize different kinds of cellulose fibers including four different nanofibrillar celluloses. The binding assay is simple and robust and may be used on both cryopreserved and paraffin-embedded tissues. The level of nonspecific staining is very low, the staining procedure is straightforward, and the assay has good sensitivity. The  $K_D$  of the EXG:CBM binding to nanofibrillar cellulose is in the order of  $10^{-8}$  M, thus in the same range as the antibody–antigen interaction. Furthermore, in contrast to many antibodies, EXG:CBM-binding is not compromised by formaldehyde treatment, and EXG:CBM recognizes both unmodified cellulose and cellulose fibers which have been modified by carboxylation and methylation (such as CF2

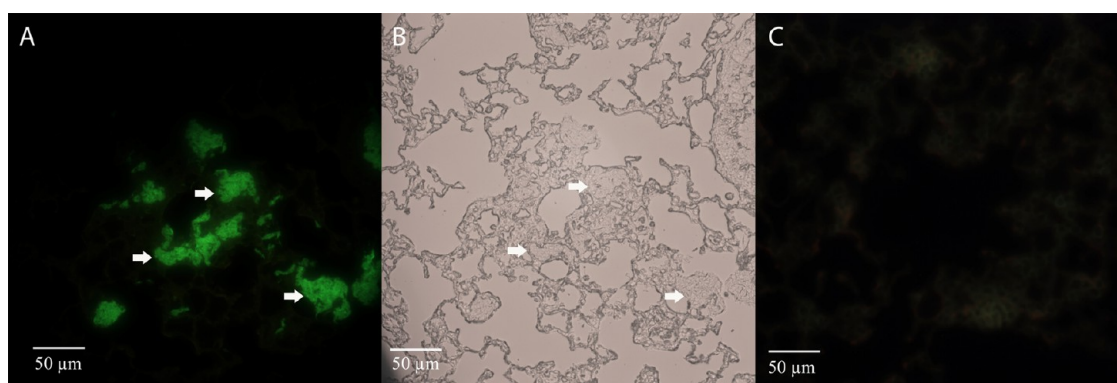


**Figure 6.** Paraffin embedded lung sections of mice exposed to CF1 or vehicle for 24 h. A: Lung section from a mouse exposed to 200  $\mu\text{g}$  of CF1 by aspiration (ASP). The section was stained with biotinylated EXG:CBM and FITC fluorescent avidin. Microscope objective is 40 $\times$ . Arrows locate cellulose fibers identified by the EXG:CBM staining. B: The same tissue section in bright field with no counterstaining. CF1 is located by arrows. Microscope objective is 40 $\times$ . C: Lung section from a vehicle-exposed mouse stained with biotinylated EXG:CBM and FITC fluorescent avidin.

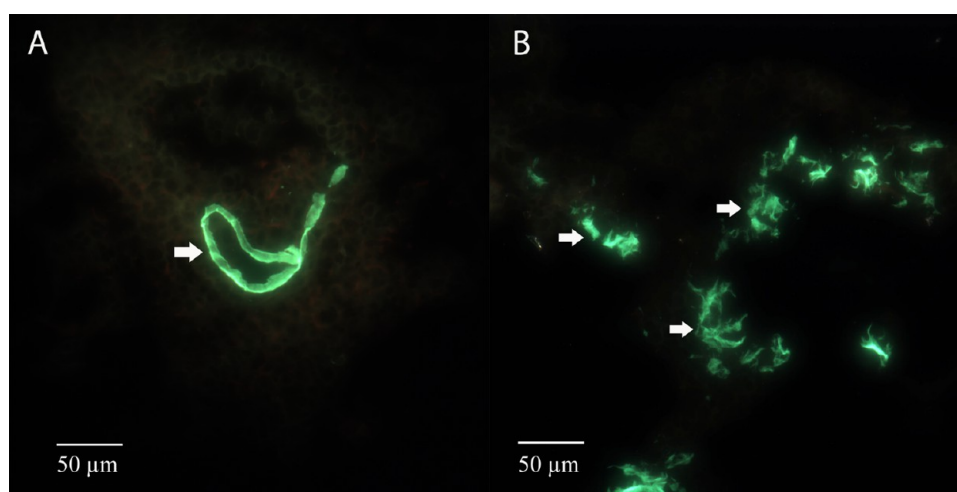


**Figure 7.** Cryopreserved lung sections of mice exposed for 24 h. A: Lung section from a mouse exposed to 200  $\mu\text{g}$  of CF3 by aspiration. The section was stained with biotinylated EXG:CBM and FITC fluorescent avidin. Microscope objective is 40 $\times$ . Arrows locate cellulose fibers identified by the EXG:CBM staining. B: Lung section from a mouse exposed to 200  $\mu\text{g}$  of CF1 by ASP. The section was stained with biotinylated EXG:CBM and FITC fluorescent avidin. Microscope objective is 40 $\times$ . Arrows locate cellulose fibers identified by EXG:CBM staining.

and CF3). Thus, the binding of EXG:CBM is quantitative and robust. The fact that paraffin embedding does not interfere with the assay furthermore opens a wide variety of possible applications including detection of cellulose fibers in preserved animal tissues, tissues from patients, and occupationally exposed individuals.

On the basis of previous investigations of the interaction of EXG:CBM with cellulosic materials, the application of EXG:CBM can likely be extended to the detection of compounds like bacterial microcrystalline cellulose, Avicel, and  $\alpha$ -chitin (a  $\beta$ -1,4 polymer of 2-*N*-acetyl-glucosamine units).<sup>10</sup> The affinity of EXG to Avicel was exploited in the present purification of EXG. The  $\beta$ -1,4-glycanase from *Cellulomonas fimi* from which EXG:CBM is derived has been shown to hydrolyze *para*-nitrophenyl- $\beta$ -xylobioside showing that the enzyme has affinity for xylans (hemicellulose) in the active site. However, this observation cannot be extended to describe the binding specificity of EXG:CBM alone.<sup>23</sup>

Inhalation of cellulose fibers in cotton dust has been associated with respiratory disease.<sup>6</sup> Wood dust has been classified as a human carcinogen that can cause adenocarcinomas of nose and paranasal sinuses and occupational exposure to wood dust is associated with highly increased risk of sinonasal

cancer.<sup>7,24,25</sup> Since there is no relevant model for testing the carcinogenicity of wood dust in animals, the carcinogenic component in wood dust is still unknown. The very long latency between exposure and cancer could indicate that long-term retention of wood-dust components is important and might point to cellulose.<sup>24</sup> A method for specific detection of cellulose is critical for understanding the distribution and retention of inhaled cellulose. The binding data for all of the studied cellulose fibers in the present study (Table 2) show quantitative binding of EXG:CBM to all of the studied cellulose fibers. The high specificity for cellulose of our detection method allows for the development of assays for quantitative and qualitative detection of nanofibrillar cellulose. The EXG:CBM was biotinylated on two sites, and both mono- and dibiotinylated EXG:CBM were detected (Figure 1B). However, a uniform double-labeling of EXG:CBM should be achievable by increasing the excess amount of NHS-biotin used.

In a study of cellulose toxicity, Cullen et al. did not succeed in locating cellulose fibers in macrophages after a 14-day inhalation exposure to cellulose fibers or after a 28 day recovery period, probably because the low refraction index of cellulose prevented its visualization in optical microscopy.<sup>24</sup> Using the



methods described herein, cellulose fibers were faintly visible in H&E staining as can be seen by comparing Figure 2A and B or Figure 3C and D. In other work, microcrystalline cellulose has been visualized with a modified Russell Movat penta-chrome stain.<sup>26</sup> However, the staining procedure was characterized as “technically challenging” by the authors due to inconsistency of the staining results and due to additional staining of tissue collagen leading to potential misinterpretations.<sup>26</sup> We believe that the presently described method is a promising tool for specific visualization of cellulose fibers in future *in vivo* experiments, due to the high specificity and robustness of the assay.

## CONCLUSIONS

In conclusion, we have described a novel, robust method for the specific detection of cellulose fibers including four different nanofibrillar celluloses. The binding to cellulose fibers was quantitative, and the method can be used to visualize cellulose in biological tissue with high sensitivity and specificity. The quantitative binding to cellulose may allow for the development of quantitative detection assays.

## AUTHOR INFORMATION

### Corresponding Author

\*Tel: +45 39 16 52 27. Fax: +45 39 16 52 01. E-mail: [ubv@nrcwe.dk](mailto:ubv@nrcwe.dk)

### Funding

Support from the European Union Seventh Framework Program (FP7/2007-2013) under the project NANoREG (A common European approach to the regulatory testing of nanomaterials), grant agreement 310584, and Danish Centre for Nanosafety, grant# 20110092173-3 from the Danish Working Environment Research Foundation, is gratefully acknowledged.

### Notes

The authors declare the following competing financial interest(s): I.W. is employed by Stora Enso, and M.N. is employed by UPM Kymmene Oyj, producers of nanofibrillar cellulose.

## ACKNOWLEDGMENTS

We thank all the technical personnel for their work. Specifically, Sauli Savukoski from FIOH for preparing and staining tissue slides with HRP-EXG:CBM and Anne Abildstrup from NRCWE for preparing and staining tissue slides with fluorescent avidin-EXG:CBM.

## ABBREVIATIONS

ASP, aspiration;  $B_{max}$ , concentration of binding sites; CF1–5, cellulose fibrillar 1–5; *E. coli*, *Escherichia coli*; EXG:CBM, carbohydrate binding module of  $\beta$ -1,4-glycanase (EXG); HCl, hydrogen chloride; H&E, hematoxylin and eosin; HRP, horseradish peroxidase; IPTG, isopropyl  $\beta$ -D-1-thiogalactopyranoside;  $K_{D1-2}$ , indicates the binding constant for 1-site binding or the 2-site binding; [L], concentration of free (not bound) EXG:CBM; NHS-biotin, N-hydroxysuccinimidobiotin; MALDI-TOF MS, matrix-assisted laser desorption/ionization–time of flight mass spectrometry; O.C.T. compound, optimal cutting temperature compound; SDS–PAGE, sodium dodecyl sulfate–polyacrylamide gel electrophoresis; TEM, transmission electron microscopy; TFA, trifluoroacetic acid

## REFERENCES

(1) Vartiainen, J., Pohler, T., Sirola, K., Pylkkanen, L., Alenius, H., Hokkinen, J., Tapper, U., Lahtinen, P., Kapanen, A., Putkisto, K.,

Hiekkataipale, P., Eronen, P., Ruokolainen, J., and Laukkanen, A. (2011) Health and environmental safety aspects of friction grinding and spray drying of microfibrillated cellulose. *Cellulose* 18, 775–786.

(2) Johnson, R. K., Zink-Sharp, A., Renneckar, S. H., and Glasser, W. G. (2009) A new bio-based nanocomposite: fibrillated TEMPO-oxidized celluloses in hydroxypropylcellulose matrix. *Cellulose* 16, 227–238.

(3) Lavoine, N., Desloges, I., Dufresne, A., and Bras, J. (2012) Microfibrillated cellulose - Its barrier properties and applications in cellulosic materials: A review. *Carbohydr. Polym.* 90, 735–764.

(4) Catalan, J., Ilves, M., Jarventaus, H., Hannukainen, K. S., Kontturi, E., Vanhala, E., Alenius, H., Savolainen, K. M., and Norppa, H. (2015) Genotoxic and immunotoxic effects of cellulose nanocrystals in vitro. *Environ. Mol. Mutagen.* 56, 171–182.

(5) Clift, M. J., Foster, E. J., Vanhecke, D., Studer, D., Wick, P., Gehr, P., Rothen-Rutishauser, B., and Weder, C. (2011) Investigating the interaction of cellulose nanofibers derived from cotton with a sophisticated 3D human lung cell coculture. *Biomacromolecules* 12, 3666–3673.

(6) Rylander, R., Schilling, R. S., Pickering, C. A., Rooke, G. B., Dempsey, A. N., and Jacobs, R. R. (1987) Effects after acute and chronic exposure to cotton dust: the Manchester criteria. *Occup. Environ. Med.* 44, 577–579.

(7) IARC (1995) Wood dust and Formaldehyde. *IARC Monogr. Eval. Carcinog. Risks Hum.* 62, 35–215.

(8) IARC (1990) Some flame retardants and textile chemicals, and exposures in the textile manufacturing industry. *IARC Monogr. Eval. Carcinog. Risks Hum.* 48, 1–278.

(9) Muhle, H., Ernst, H., and Bellmann, B. (1997) Investigation of the durability of cellulose fibres in rat lungs. *Ann. Occup. Hyg.* 41 (Suppl 1), 184–188.

(10) Ong, E., Gilkes, N. R., Miller, R. C., Jr., Warren, R. A., and Kilburn, D. G. (1993) The cellulose-binding domain (CBD(Cex)) of an exoglucanase from *Cellulomonas fimi*: production in *Escherichia coli* and characterization of the polypeptide. *Biotechnol. Bioeng.* 42, 401–409.

(11) Xu, G. Y., Ong, E., Gilkes, N. R., Kilburn, D. G., Muhandiram, D. R., Harris-Brandts, M., Carver, J. P., Kay, L. E., and Harvey, T. S. (1995) Solution structure of a cellulose-binding domain from *Cellulomonas fimi* by nuclear magnetic resonance spectroscopy. *Biochemistry* 34, 6993–7009.

(12) Tholstrup, J., Oddershede, L. B., and Sorensen, M. A. (2012) mRNA pseudoknot structures can act as ribosomal roadblocks. *Nucleic Acids Res.* 40, 303–313.

(13) Lauritsen, I., Willemoes, M., Jensen, K. F., Johansson, E., and Harris, P. (2011) Structure of the dimeric form of CTP synthase from *Sulfolobus solfataricus*. *Acta Crystallogr., Sect. F: Struct. Biol. Cryst. Commun.* 67, 201–208.

(14) Chaplin, M. F., and Kennedy, J. F. (1986) *Carbohydrate Analysis: A Practical Approach*; IRL Press, Oxford.

(15) Creagh, A. L., Ong, E., Jervis, E., Kilburn, D. G., and Haynes, C. A. (1996) Binding of the cellulose-binding domain of exoglucanase Cex from *Cellulomonas fimi* to insoluble microcrystalline cellulose is entropically driven. *Proc. Natl. Acad. Sci. U. S. A.* 93, 12229–12234.

(16) Muhlfeld, C., Rothen-Rutishauser, B., Vanhecke, D., Blank, F., Gehr, P., and Ochs, M. (2007) Visualization and quantitative analysis of nanoparticles in the respiratory tract by transmission electron microscopy. *Part. Fibre Toxicol.* 4, 11.

(17) Nisman, R., Dellaire, G., Ren, Y., Li, R., and Bazett-Jones, D. P. (2004) Application of quantum dots as probes for correlative fluorescence, conventional, and energy-filtered transmission electron microscopy. *J. Histochem. Cytochem.* 52, 13–18.

(18) Kobler, C., Saber, A. T., Jacobsen, N. R., Wallin, H., Vogel, U., Qvortrup, K., and Molhave, K. (2014) FIB-SEM imaging of carbon nanotubes in mouse lung tissue. *Anal. Bioanal. Chem.* 406, 3863–3873.

(19) Kobler, C., Poulsen, S. S., Saber, A. T., Jacobsen, N. R., Wallin, H., Yauk, C. L., Halappanavar, S., Vogel, U., Qvortrup, K., and Molhave, K. (2015) Time-dependent subcellular distribution and effects of carbon nanotubes in lungs of mice. *PLoS One* 10, e0116481.

(20) Husain, M., DSaber, A. T., Guo, C., Jacobsen, N. R., Jensen, K. A., Yauk, C. L., Williams, A., Vogel, U., Wallin, H., and Halappanavar, S. (2013) Pulmonary instillation of low doses of titanium dioxide nanoparticles in mice leads to particle retention and gene expression changes in the absence of inflammation. *Toxicol. Appl. Pharmacol.* 269, 250–262.

(21) Mercer, R. R., Scabilloni, J. F., Hubbs, A. F., Battelli, L. A., McKinney, W., Friend, S., Wolfarth, M. G., Andrew, M., Castranova, V., and Porter, D. W. (2013) Distribution and fibrotic response following inhalation exposure to multi-walled carbon nanotubes. *Part. Fibre Toxicol.* 10, 33.

(22) Halappanavar, S., Saber, A. T., Decan, N., Jensen, K. A., Wu, D., Jacobsen, N. R., Guo, C., Rogowski, J., Koponen, I. K., Levin, M., Madsen, A. M., Atluri, R., Snitka, V., Birkedal, R. K., Rickerby, D., Williams, A., Wallin, H., Yauk, C. L., and Vogel, U. (2015) Transcriptional profiling identifies physicochemical properties of nanomaterials that are determinants of the in vivo pulmonary response. *Environ. Mol. Mutagen.* 56, 245–264.

(23) Gilkes, N. R., Claeysens, M., Aebersold, R., Henrissat, B., Meinke, A., Morrison, H. D., Kilburn, D. G., Warren, R. A., and Miller, R. C., Jr. (1991) Structural and functional relationships in two families of beta-1,4-glycanases. *Eur. J. Biochem.* 202, 367–377.

(24) Cullen, R. T., Searl, A., Miller, B. G., Davis, J. M., and Jones, A. D. (2000) Pulmonary and intraperitoneal inflammation induced by cellulose fibres. *J. Appl. Toxicol.* 20, 49–60.

(25) Acheson, E. D., Pippard, E. C., and Winter, P. D. (1984) Mortality of English Furniture Makers. *Scand. J. Work, Environ. Health* 10, 211–217.

(26) Sigdel, S., Gemind, J. T., and Tomashefski, J. F., Jr. (2011) The Movat pentachrome stain as a means of identifying microcrystalline cellulose among other particulates found in lung tissue. *Arch. Pathol. Lab Med.* 135, 249–254.

#### ■ NOTE ADDED AFTER ASAP PUBLICATION

This paper was published ASAP on August 6, 2015, with an error in the spelling of the name of author Harri Alenius. The corrected version was reposted on August 17, 2015.